April 1986 LRP 289/86

Papers contributed to the
13th EUROPEAN CONFERENCE ON CONTROLLED
FUSION AND PLASMA PHYSICS by the TCA Group

Schliersee, Germany, April 1986

A REVIEW OF ALFVEN WAVE HEATING

G. Besson, A. de Chambrier, G.A. Collins, B. Joye, A. Lietti, J.B. Lister, J.M. Moret, S. Nowak, C. Simm, H. Weisen

Presented by J.B. Lister

Centre de Recherches en Physique des Plasmas
Association Euratom - Confédération Suisse
Ecole Polytechnique Fédérale de Lausanne
21, Av. des Bains, CH-1007 Lausanne / Switzerland

ABSTRACT

This paper reviews the experimental status and recent advances in Alfvén Wave Heating (AWH). We discuss the underlying physics of Alfvén Wave Heating, as seen by the experiments. The use of Alfvén Waves for plasma diagnosis is discussed. The results of plasma heating on TCA are summarized. Apparent changes in the current profile are inferred, caused by changes in the evolving Alfvén wave spectrum excited. The implications for AWH on larger devices are mentioned.

KEYWORDS

Alfvén Wave Heating; Tokamak; Kinetic Alfvén Wave; Profile Control; Antenna System; Plasma Diagnostics; TCA.

INTRODUCTION

In this paper we shall review the recent experimental results obtained in Alfvén Wave Heating (AWH). The early experimental results have already been reviewed by Shohet (1978), and we shall not repeat that survey. An overview of the extensive theoretical work in this frequency range is beyond this paper, and the current status has been very recently reviewed by Appert and colleagues (1986). We shall review the theoretical basis of AWH from the viewpoint of the experimental observations made, and shall, in fact, discover that most of the important concepts manifest themselves in the results.

Results on plasma formation in the Alfvén wave frequency range on the OMEGA and URAGAN-3 devices have been reported by Shvets and co-workers (1986). Experimental results on current drive in the R-O stellarator were reported by Demirkhanov and co-workers (1981, 1983), and this topic was also discussed by Sidorov and co-workers (1983).

Results of bulk plasma heating since Shohet's review paper are restricted to those obtained on TCA. We shall summarize these heating results and the importance of the excited spectrum. The new generator on TCA has enabled us to increase the delivered power to over 500 kW. We discuss the large increase in plasma density during the rf pulse, estimating the fraction due to impurities to be small. The problem of impurity influx, although reduced, still causes a large radiated power problem at the higher densities in TCA ($\bar{n}_e > 6 \times 10^{19} m^{-3}$). A considerable amount of work has been carried out on the edge plasma changes during rf heating, and the major results have been described by de Chambrier and colleagues (1984a).

The excited spectrum evolves as a result of the increasing density. During this evolution we have observed discontinuous behaviour of several parameters, at the thresholds of new AW

continua. It now appears that a change in current profile may be responsible for this behaviour. Such changes may also be responsible for our present power limitation.

The improved understanding of the launching of Alfvén waves has led to greater confidence in the design of antennae for a large device, and we briefly discuss the extrapolation of AWH to a more powerful tokamak.

THE PHYSICS BEHIND ALFVEN WAVE HEATING

In this section we review the experimental observations which have led to a better understanding of the importance of the different elements of the underlying physics, particularly of the requirements of AWH antennae. We nevertheless begin with a brief theoretical resumé of the Alfvén Wave spectrum.

The Alfvén Wave Resonance

The Alfvén wave can be excited in an inhomogeneous plasma if the condition $\omega = [1/v_A{}^2 k_{//}{}^2 + 1/\omega_{ci}{}^2]^{-1/2}$ is satisfied. In periodic cylindrical geometry the resonant frequency $\omega(r)$ is a function of radius since $v_A(r) = B_\emptyset/[\mu_0 \rho(r)]^{1/2}$ and $k_{//}(r) = [n+m/q(r)]/R$ where n,m are the toroidal and poloidal mode numbers and $\rho(r)$, $q(r)$ are the local values of mass density and safety factor. In the context of mhd theory, this describes a continuous spectrum of "shear" Alfvén waves, extending from a threshold value ω_{min} close to the magnetic axis to a maximum value at the plasma edge. This is illustrated (as a function of line-averaged density) in Fig. 1 for typical TCA parameters (a =0.18m, R =0.61m, $B_\emptyset$ = 1.5T, q(a) = 3.2, q(0) = 0.95) calculated with parabolic power profiles of density and current in a deuterium plasma for n = 2, m = -1,0,1,2 and a frequency of 2.5 MHz. Closer to reality, kinetic theory including finite temperature effects does not just predict the large localised oscillating fields characteristic of the "shear" Alfvén wave in mhd, but also indicates that, as long as the resonance position r_A is not too close to the edge, a "kinetic" Alfvén wave propagates from r_A towards the centre. In a typical tokamak plasma the dissipation is expected to be mostly via electron Landau damping.

Alfvén Wave Antennae

Historically, extremely large structures were employed to specify the n,m of the oscillating fields external to the plasma column (Shohet, 1978). Often these were helical windings which completely enclosed the toroidal volume. On some experiments it seemed most logical to excite the Alfvén wave via its dominant wavefield component, perpendicular to the static field, so longitudinal antennae were used. Borg and colleagues (1985) have shown that such an antenna will excite a wave localised to the antenna radius. Kirov and colleagues (1984) have reported such a wave in the plasma periphery driven by the longitudinal current elements of their helical antenna, and, although they comment that this may be useful for plasma pre-ionisation and preliminary heating, they are not alone (Taylor and others, 1984) in observing advantages of antennae with perpendicular currents.

In fact there is every advantage in antennae which maximise the magnetic pressure modulation $\underline{b}.\underline{B}$ at the plasma boundary. Coupling to the Alfvén wave in the plasma (particularly if r_A is near the centre) is most efficient when the frequency is close to a natural mode of the plasma-vacuum system. In AWH applications this corresponds to the lowest frequency mode of the fast wave. The presence of the Alfvén wave resonance in the plasma strongly damps this mode, often called a "surface wave", so that there is a broad frequency range over which efficient coupling is possible.

On TCA, eight antenna groups with purely poloidal current elements are used. A group is placed above and below the plasma in each quadrant of the torus. By phasing the currents in the different groups we can define the principal n,m modes excited. The width of the antenna groups has little effect on the lower-n components, the main purpose being to reduce the inductance so as to give lower voltages for a given delivered power. For 500 kW delivered there is typically 500 A rms in each antenna group, distributed over six parallel conductors, giving an oscillating voltage of 250 V rms. At the relatively low frequency used, the evanescence in the vacuum layer is very small, so the antenna-plasma spacing is

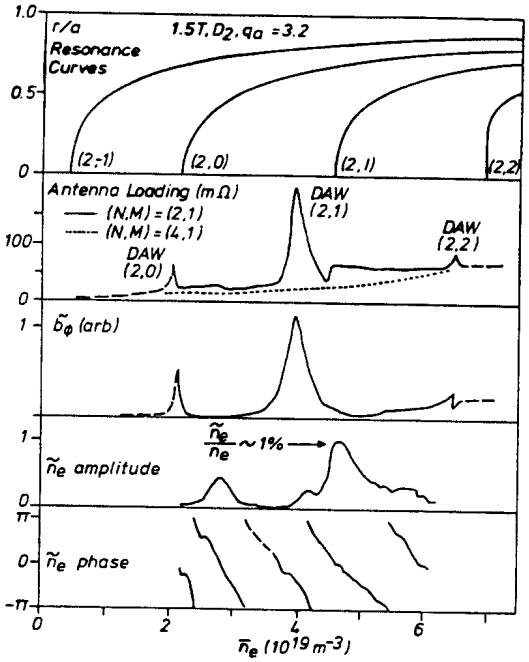

Fig. 1 The Alfvén wave spectrum excited on TCA.

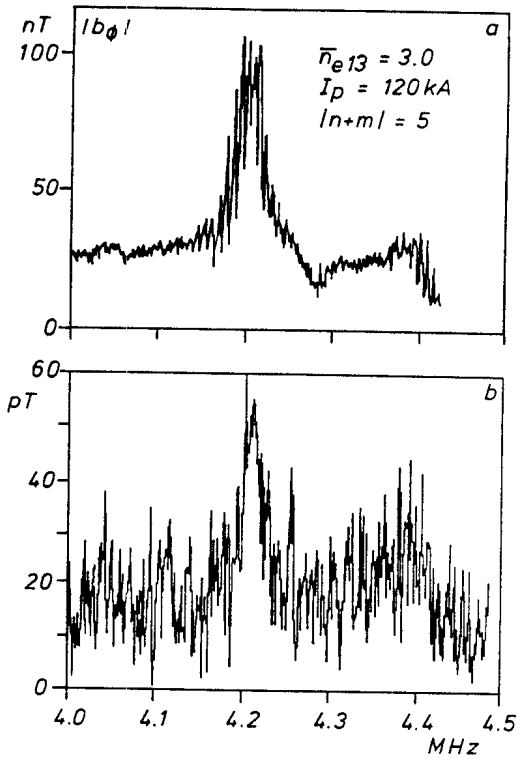

Fig. 3 Discrete Alfvén wave excited by random magnetic noise in TCA.

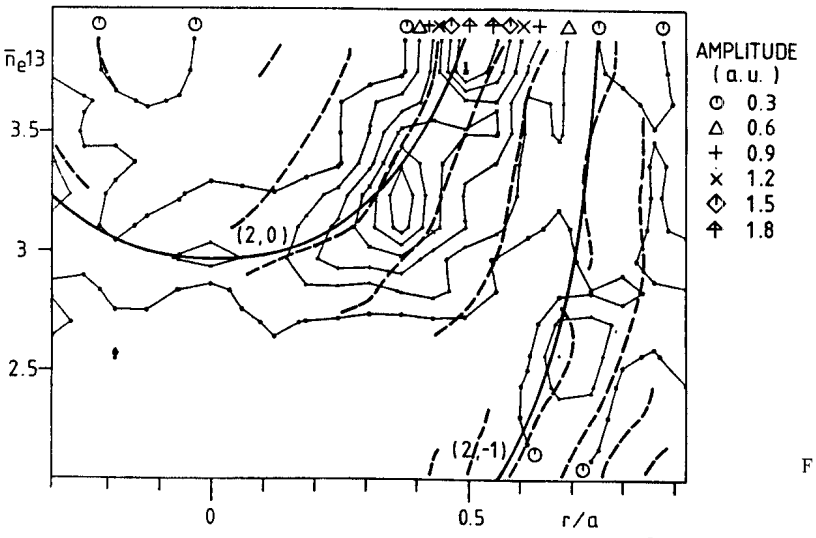

Fig. 4 Evolution of the radial structure of the driven density oscillations, as the density increases.

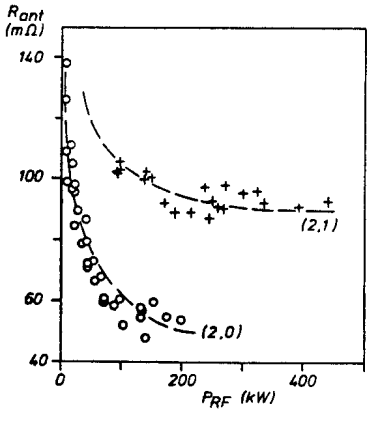

Fig. 2 Independence of the antenna coupling on the delivered power at higher powers.

not critical. The main reduction in coupling is produced by image currents in the vessel wall. How much reduction in coupling can be tolerated depends on the strength of the surface wave mode. The antenna feeds (vertical in the case of TCA) also contribute to the mixture of modes excited. Calculations by Hofmann, Appert and Villard (1984) and Ross and colleagues (1986) have shown that tilting the antennae by quite small angles from their purely poloidal position could lead to preferential excitation of modes of one sign of helicity, due to the effect of the feeds. Tilting the antennae will be tested on TCA in the near future.

A related question is the need for an electrostatic screen. Due to the low rf voltages, TCA usually operates without any form of shield. Lateral screens intended to inhibit current flow in the residual plasma between antenna groups caused a significant reduction in coupling, presumably by blocking the wavefield of the surface wave. Of course even poloidal current elements will launch some waves in the plasma periphery and this may be the cause of the increase in antenna loading normally seen at low powers - Fig. 2. Reducing the density of the scape-off layer at the antenna, as was achieved down to the lowest powers with lateral screens, and in all cases with more than 80kW delivered, results in a constant loading with power.

On TCA the antenna is matched to the generator by a simple ringing circuit which is placed rather inefficiently at a distance of 5 m from the antenna. Losses in the circuit are subtracted from the total power delivered measured at the tuning capacitor. We refer to the power delivered to, and the loading provided by the plasma itself, following this subtraction.

The Measured Spectrum

Details of the Alfvén wave spectrum as seen on TCA have been fully discussed by Collins and colleagues (1986). A typical antenna loading curve (averaged over the 8 groups) is shown in Fig. 1. The antennae were phased to excite modes with $n = \pm 2, \pm 6, \ldots$ and $m = \pm 1, \pm 3, \ldots$. Such a phasing is labelled $N = 2$, $M = 1$. The rf power was 400 kW and other parameters are as for Fig. 1(a). Firstly we note three resonance peaks of relatively high antenna loading at densities just below the thresholds of the $n = 2$, $m = 0,1,2$ continua. These form part of the Discrete Alfvén Wave (DAW) spectrum. The featureless parts of the spectrum around each DAW peak is interpreted as being due to the sum of the various continua.

The Discrete Alfvén Wave

The DAW, first reported on TCA by de Chambrier and colleagues (1982), is the low frequency counterpart of the ion-cyclotron wave and owes its existence, as ω/ω_{ci} tends to zero, to the presence of the plasma current (Appert and colleagues, 1982). It is a global mode of the Alfvén wave and its structure has been measured by interferometric measurements of its density fluctuations by Evans and colleagues (1984). On TCA, our study of the DAW has been mainly with magnetic probes outside the limiter radius. A typical measurement of the toroidal component $\tilde{b}_\phi$ is shown in Fig. 1.

Since it is easily observed, the DAW spectrum has been of considerable use in investigating spectral purity and in identifying the excited modes (de Chambrier and colleagues, 1984b). Immediately evident from Fig. 1, modes are present in the spectrum which do not exist in the $N = 2$, $M = 1$ antenna structure. In particular we see DAWs associated with the $n = 2$, $m = 0$ and $n = 2$, $m = 2$ modes. Appert and colleagues (1985) have demonstrated that the excitation of these peaks and of their associated continua is due to toroidal coupling between different cylindrically pure waves.

While indicating a lack of poloidal purity, the DAW spectrum also reveals the extremely high toroidal purity possible. In Fig. 1 the $N = 4$, $M = 1$ loading spectrum is also shown (dotted) and none of the peaks observed with $N = 2$ are present. This emphasises the phase coherence of the excitation. A further observation made with the DAW spectrum is the removal of the degeneracy between two waves of the same helicity (eg. $n = 2$, $m = 1$ and $n = -2$, $m = -1$) (de Chambrier and colleagues, 1984b). The dominant DAWs always have $m \leq 0$ and Cramer and Donnelly (1983) indicate that this is due to ion-cyclotron effects on the surface wave. In addition calculations have shown the dominance of $m = -1$.

Recently we have investigated the use of the DAW spectrum for diagnostic purposes, particularly to measure central current and mass densities, described in detail by Collins, Lister and Marmillod (1986). Less than 10 W is necessary to obtain well-defined peaks in the wavefield, with a heterodyne detection system. The DAW frequencies (up to n = 8) are monitored either by rapidly sweeping the oscillator frequency or by tracking a given peak. Such a system has been used on TCA to measure the effective mass during impurity injection and to estimate q(0) over a wide variety of ohmic discharges; it is also installed on PETULA to provide information on current profile changes during lower-hybrid current drive. An interesting observation first made on PETULA was that of a DAW peak excited by magnetic noise. Fig. 3 is an example from TCA, (a) driven and (b) random noise excited.

The Continua and the Kinetic Alfvén Wave

As seen in Fig. 1 the continua provide relatively little information outside the plasma column. The fact that certain antenna phasings can produce almost no antenna loading when no major continuum is present shows that we measure the coupling to the mixture of Alfvén wave modes resonant at a particular frequency. Other experiments have not seen such clear evidence of continua loading, nor of narrow DAW peaks, and we attribute this to the use of longitudinal antennae (Oakes and colleagues, 1985) and/or to the relatively low power used. It should also be noted that the continuum loading on TCA is strongly dependent on plasma current, reducing markedly as the current is decreased. This may also help to explain the disparity with other experiments.

In colder, more resistive plasmas, probes have been used to study the large-amplitude oscillating fields associated with the resonance (Kirov, Ruchko and Sukachov, 1980; Tsushima, Amagishi and Inutake, 1982; Withespoon, Prager and Sprott, 1984; Kirov and colleagues, 1984). In most of these cases the resistive damping seemed to determine the observed amplitudes although finite temperature effects were invoked in the experiments of Shvets and colleagues (1986) who also reported saturation of the amplitude as the power increased. On TCA, the intallation of a phase-contrast interferometer (Weisen, 1985) has revealed the presence of density fluctuations associated with the continua (Behn and colleagues, 1986). In Fig. 1 we show the amplitude and phase of the density fluctuations at a radius of r/a = 0.4 as a function of line-averaged density in the standard conditions. Although localised to the resonance position, the fluctuations are associated with an inward propagating wave. We have confirmed the appearance and disappearance of these fluctuations when changes are made to the excitation mode. In Fig. 4 we have plotted $|n_e|$ as a function of radius showing the resonances associated with the n = 2, m = 0 and -1 continua, also indicating radii separated by 180° of phase. The propagation direction, wavelength and damping length of these fluctuations corespond to those of the Kinetic Alfvén Wave (KAW) as predicted by Hasegawa and Chen (1975).

Summary

The question of which theoretical approximation is valid for AWH has long been debated among the experts. In this section we have shown that toroidal geometry, the presence of current, ion-cyclotron effects, and finite electron temperature must all be included to explain the experimental observations. It is a widely held view that AWH is excessively complicated. This fallacy arises from the fact that other heating methods are forced to rely on simplified models neglecting some of the complex physics involved. An apparent simplicity is thus generated. It is the "almost-solvable" nature of the whole AWH problem which provides its apparent complexity and challenge.

BULK PLASMA HEATING ON TCA

The New RF Generator

The original oscillator has been replaced by a frequency tracking amplitude controlled generator described by Lietti and Besson (1986). Eight final stage amplifiers each with two triodes in push-pull are capable of delivering 3MW total into a dummy load. Up to now full use has not been made of the capabilities of the generator which is only just in service.

We have used frequency programming over a narrow range, and the power programming capability. It is expected that full exploitation will be possible in Summer 1986.

Heating of the Electrons

Early results from TCA showed up an increase in the central electron temperature (de Chambrier and colleagues, 1983). An increase in impurity concentration normally supresses a decrease in loop voltage, only convincingly seen in a series with fresh SiC-coated limiters and side-screens (de Chambrier and colleagues, 1984c). Evidence of a peaked deposition profile comes from the strongly enhanced sawtooth activity (de Chambrier and colleagues, 1985) summarized in Fig. 5 for several spectral positions. The value of $1.5 \cdot n_e(0) \cdot dT_e(0)/dt$ reached 3.4 W/cm^3, for an estimated ohmic power of 1.5 W/cm^3 ($q(0) \sim 0.95$). A peaking factor $Prf(0)/\langle Prf \rangle$ of 5-8 is inferred.

Changes in the sawtooth frequency are provoked by the rf power. Figure 6 show such a case in which the frequency increases by 50% near an AW threshold. Other cases are seen in which the frequency decreases, but which are less conclusive since the increasing density and its also tend to depress the frequency. This frequency change is likely to be associated with a change in current profile.

Supporting evidence for an effective transfer of rf power to the electrons comes from the early radiated power profiles with high power rf and metallic contamination. In Fig. 7 we show an old and a recent radiated power profile and the evolution of density and central radiated power. In Fig. 7 we show the fractional radiated power Prad/(Prf+Poh), as a function of total power, increasing to 60% for 1 MW of total power input. The maximum power loss on axis is 1.0 W/cm^3. The peakedness of the early radiated power profiles implies a peaked deposition profile. The origin of this core heating, when the resonance layer is assumed to be at $q>1$, is considered to be the observed inwardly propagating Kinetic Alfvén Wave which may deposit energy at smaller radii than the resonance layer.

Ion Heating

The first heating results from TCA showed a considerable ion temperature increase (Bugmann and colleagues, 1981). The interpretative problem has been to differentiate between an increase in T_i due to the density increase, or an impurity increase (indirect heating) and one obtained directly. Behn and colleagues (1984) showed that T_i exceeded its equivalent ohmic value during the density increase. The attainment of a steady density will enable us to increase the confidence in this interpretation.

Increase in Plasma Density

A density increase during the rf pulse was observed during the first experiments on TCA and has so far defied control. The fact that it appeared in conjunction with an allround decrease in H_α light emission (Behn and colleagues, 1984), together with a marked dependence on the excited spectrum, led to the suggestion that an increase in particle confinement was produced. The low energy neutral flux measured by charge exchange analysis does not increase during the rf pulse, in comparison with the large increase during ICRF heating, for which enhanced recycling is usually invoked. Although the increase is a reducing function of target plasma density, the rise persists up to the normal density limit at high power. When operating within 5% of the ohmic density limit, the plasma disrupts at the end of the rf pulse.

The detailed study of the effects of the spectrum (Collins and colleagues, 1985) was made difficult by the inability to obtain a steady state. It is to be hoped that the use of the long rf pulses from the new generator, and the long plasma current being commissioned, will allow the establishment of a steady state. The composition of the density increase was already discussed by these authors. Bolometric measurements showed that no impurity mix could account for the full increase, the radiated power not increasing by a large enough amout. The effective mass diagnostic similarly reached the conclusion that a large fraction of the increase must be composed of the filling gas. Both measurements suggest that 20-30% only may be due to new impurities, of which a fraction must be metallic, to produce the peaked radiated power profile.

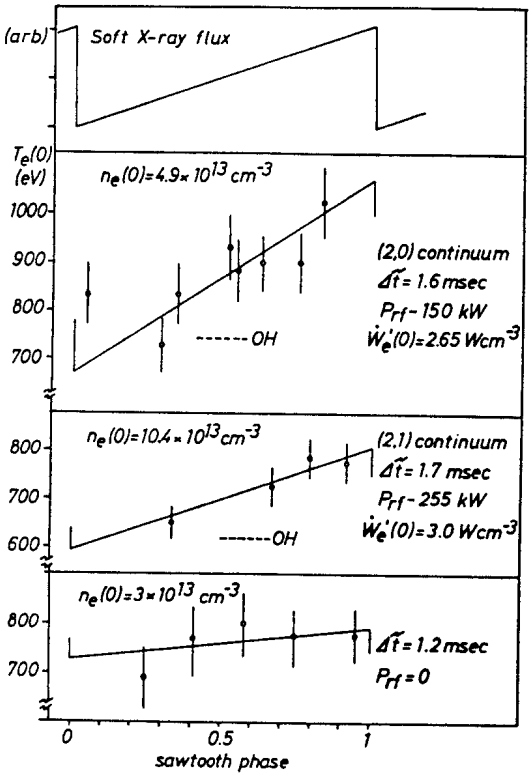

Fig. 5 T_e sawtooth excursions during the rf pulse.

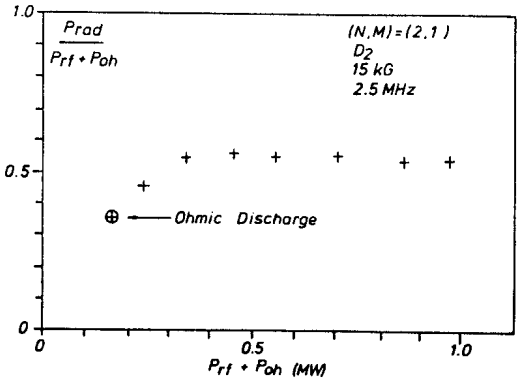

Fig. 8 Fractional radiated power as function of total power.

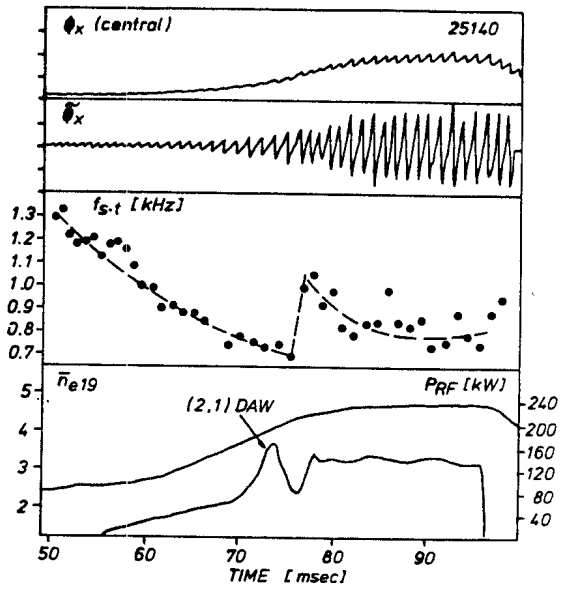

Fig. 6 Change in sawtooth frequency at an AW threshold.

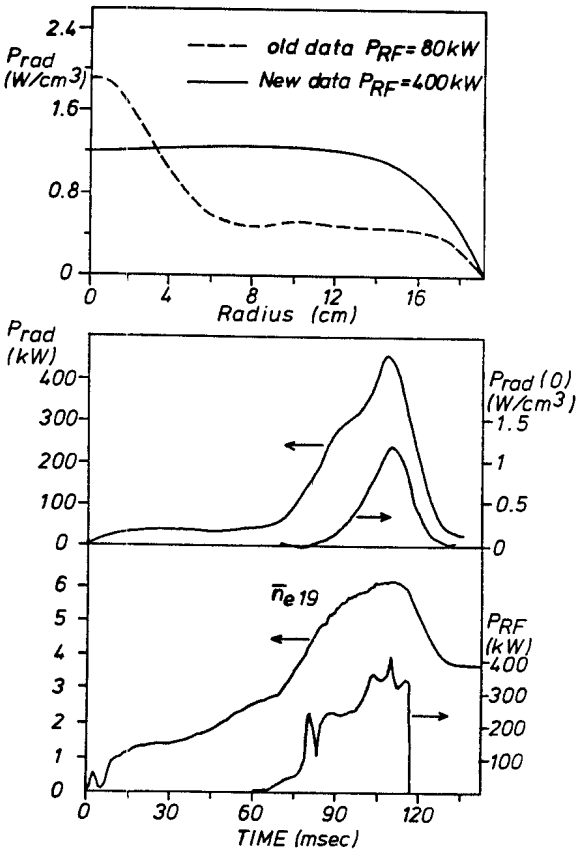

Fig. 7 Radiated power profiles and evolution of density and radiated power on axis.

Summary

Experiments on TCA have shown a substantial transfer of rf power to the plasma, half of which is presently radiated away. The peaked radiated power profile and the large gradient of the sawteeth both suggest a peaked power deposition profile, and the energy vector to within the q = 1 surface may be the observed Kinetic Alfvén Wave. An impurity influx remains, although reduced. The question whether AWH has a more severe problem than other heating methods cannot be addressed in TCA. It is clear that as the size of ICRF heating experiments increased the relative impact of impurity increase has diminished. It may well be that the small plasma volume on TCA ($0.4m^3$) is responsible for the relative importance of the problem. Only tests on a larger device will answer this question.

The question of heating efficiency and confinement has not been addressed here. The significant increases in β_p + li/2, up to 0.5, are encouraging. However the large increase in plasma density, up to 300% for a low density target plasma at high power, confuses any serious analysis of efficiency at present. The achievement of a stationary state will go a long way to making these studies meaningful.

CURRENT PROFILE EFFECTS

Since the Alfvén Wave resonance layers are magnetic surfaces, it has long been conjectured that profile control should be possible using AWH, for example by Degtyarev and colleagues (1984). We present here the first experimental results from TCA which indicate that this may well be the case.

Change in li

Abrupt changes in the temporal evolution of the equilibrium value of β + li/2 have often been observed in TCA. In general we have tried to avoid these by a variety of operational tricks, to obtain a more controlled evolution. Recently we have observed cases in which a small rise in β + li/2 early in the rf pulse was followed by a pronounced and maintained droop, as shown in Fig. 9, taking β + li/2 to well below its starting value. In the absence of a reliable estimate of β_p from a diamagnetic measurement, we estimate the range of β_p from the measured increases in $n_e(r)$, $T_i(0)$, and the maintained electron temperature. The ohmically heated plasma energy content at the increased density is also evaluated. This range is shown in the figure. Together with β + li/2 this leads us to a range of values for the evolution of the internal inductance li, which must be decreasing by 0.4 - 0.6, corresponding to a substantial flattening of the current profile. The central soft X-ray diodes show that the sawtoothing activity is maintained. In Fig. 9 we also show the position in the spectrum, from the antenna loading curve. The abrupt change in the behaviour of li occurs close to the (n,m) = (2,0) AW threshold.

During the early part of the rf pulse the rate of increase of β + li/2 is often extremely rapid, whereas the diamagnetic signals evolve more slowly. It is therefore quite possible that different parts of the excited AW spectrum can produce current peaking. The lack of a steady density during the short rf pulses, < 60 msec at present, do not allow us to say whether the changed profiles are maintainable in a steady state.

Change in MHD Behaviour and Power Limits

The increased probability of disruption near new AW thresholds was already reported on TCA by Appert and colleagues (1984a). We regularly observe changes in the middle frequency mhd activity, dominated by the (m,n) = (2,1) mode, near the AW thresholds, and an example is shown in Fig. 10, near the (n,m) = (2,0) DAW. The mhd signal increases until the new AW layer appears, estimated by the vertical arrow, when the activity decreases. The increase is certainly due to the sensitivity to the local current profile. The decrease may be for either of two reasons. The outer (n,m) = (2,-1) resonance layer may have crossed q = 2 with the increasing density, and be stabilising, as discussed for ECRH by Alikaev and Razumova (1985). Alternatively the new threshold, changing the power deposition profile near the centre, may have a stabilising influence. The frequency tends to increase following the amplitude reduction.

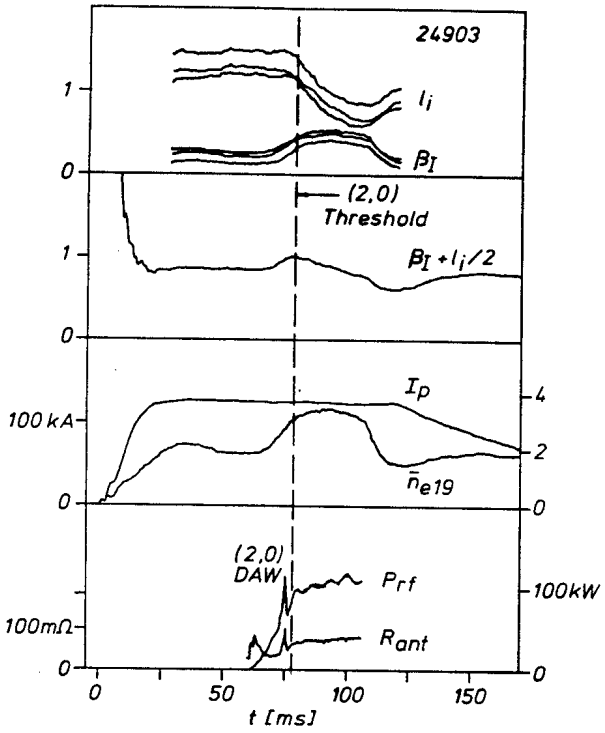

Fig. 9 Discontinuous evolution of $\beta + \ell_i/2$, β, ℓ_i.

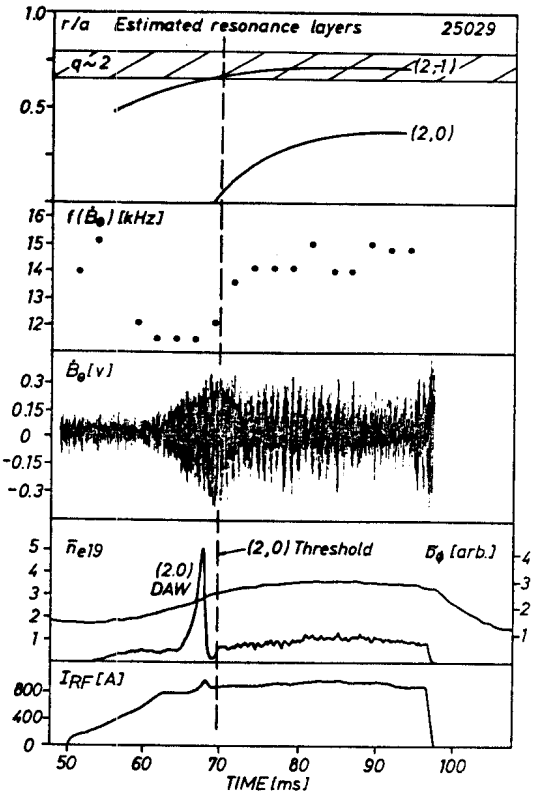

Fig. 10 Changes in the (m,n) = (2,1) signal near an AW threshold. The estimated resonance layers are indicated.

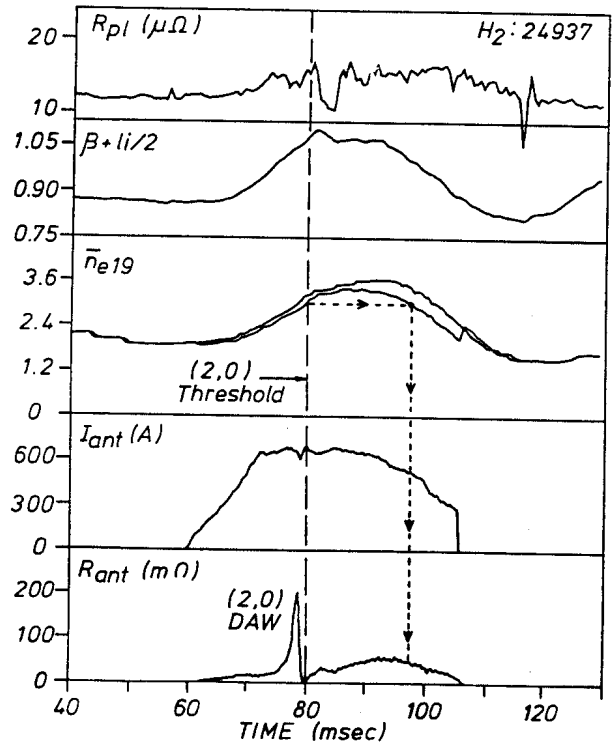

Fig. 11 Sweeping through the AW spectrum in both directions, around the (n,m) = (2,0) DAW.

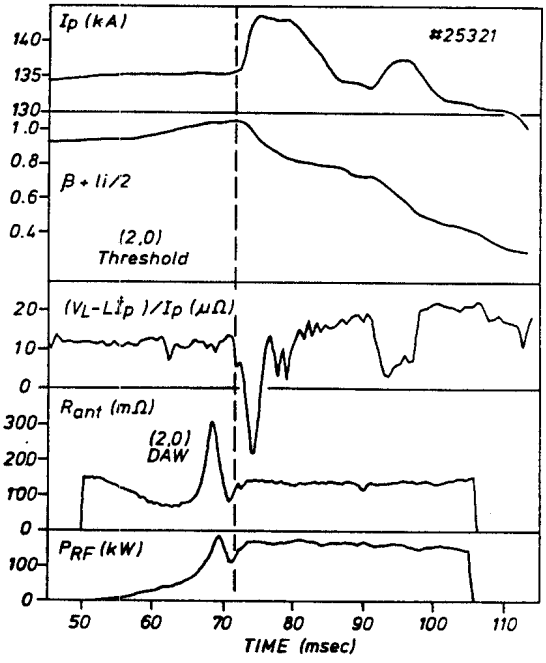

Fig. 12 An example of current surging during the RF pulse.

We now interpret these changes in terms of the resonance surface which is already excited, the (n,m) = (2,-1) layer, which is close to the guessed q = 2 surface position, shown in Fig. 10. It seems to us now that the crossing of q = 2 is leading to the charge in li, and not the new threshold. The outer soft X-ray signals (r > 10cm) show a sudden increase at this time.

Above a certain level of mhd activity, the amplitude never decreases again, and a disruption ensues. Although disruptions occasionally occur during the rf pulse at other densities - other spectral positions - the majority occur close to the spectral thresholds, and consequently limit the rf power delivered in these zones. It is therefore to be hoped that correct frequency programming of the rf generator will avoid these disruptions and increase the delivered power, by jumping over the difficult zones in the spectrum. As a result of this source of power limitation, we have delivered different rf powers in different parts of the spectrum, namely 400 kW at the (n,m) = (2,0) DAW; 500 kW at the (n,m) = (2,1) DAW; 295 kW in the (n,m) = (2,0) continuum and 570 kW in the (n,m) = (2,1) continuum.

Change in the DAW Excitation

Programming of the rf power and frequency in TCA has enabled us to move forwards and then backwards in the AW spectrum in one plasma discharge, illustrated in Fig. 11. The toroidally coupled (n,m) = (2,0) DAW is crossed during the initial density rise, shown up by the narrow peak in the b_0 rf wavefield amplitude. The spectral position is given by $\bar{n}_e f^2/f_o^2$, the dashed curve, and the drop in frequency during the rf pulse accentuates the subsequent reduction in density. The resonant $\bar{n}_e f^2/f_o^2$ was crossed on the descent, shown by the horizontal and vertical dotted lines, but no pronounced (n,m) = (2,0) resonance peak was seen in the wavefield amplitude. It is known from numerical computations by Villard (1984) that the excitation of this eigenmode is extremely sensitive to the current profile, requiring peaked profiles to be strongly excited. We therefore accept that a flattening of the current profile around the (n,m) = (2,0) DAW zone of the spectrum has caused the disappearance of the eigenmode. Between the observation and the disappearance of the eigenmode, the trace $\beta + li/2$ has suffered a sharp drop at the same time that Rpl = $(V_L - L_p\dot{I}_p)/I_p$ has a negative spike. This estimate of Rpl contains the term $10^{-7} \cdot R_o \cdot li$ when V_L is the surface voltage. The negative spike in Fig. 11 then corresponds to a drop in the internal inductance.

Current Surging Induced by the RF Power

To complete the phenomenology associated with current profile changes, we show in Fig. 12 one of the rare examples of current surging seen on TCA. This has only ever been seen during the rf pulse, and we must therefore relate it to the rf power. The plasma current suddenly increases, by 15 kA in one case, and the calculated value of $(V_L - L_p\dot{I}_p)/I_p$ decreases as shown. This change is reminiscent of a non-terminal disruption and can be interpreted as a redistribution of the current channel. In the example shown, the current surge occurred twice during the rf pulse, both times at the same spectral position, borne out by the measurements of the synchronous density modulation. It seems clear that this is an extreme case of current profile modification provoked by the AW spectrum. Unfortunately it cannot be systematically studied, since we have not yet learned how to induce this behaviour voluntarily.

Summary

The importance of the location of the resonance surfaces is becoming more and more evident as the TCA experiment evolves. The observations of changes in li, spikes in Rpl, and the disappearance of an eigenmode all suggest a modification to the current profile. This modification is regularly reproducible, is caused by particular zones of the AW spectrum, and is therefore controllable. Certain zones increase the (m,n) = (2,1) mhd activity, producing our present power limitation at these points in the spectrum. We conjecture that the modification of the current profile may be responsible for much of the discontinuous macroscopic behaviour previously associated with the arrival of a new AW threshold (Behn and colleagues, 1984; Appert and colleagues, 1984a,b).

ALFVEN WAVE HEATING ON LARGER DEVICES

The successful absorption of the rf power by the plasma and the newly apparent possibilities of current profile control encourage us to discuss the extrapolation of AWH from TCA to a larger device. Since the size of the machine and toroidal field both tend to increase, the resonant frequency does not vary dramatically. If we work at a density which is a given fraction of the density limit (~B/R) then the frequency scales as $\sqrt{(B/R)}$ for a given Alfvén mode. It has often been conjectured that the losses in the antenna and wall would exceed the plasma loading, as was the case with TTMP. In TCA we estimate the equivalent losses in the vacuum part of the antenna circuit as typically 20-25 mΩ at 2.5 MHz, compared with typically 130 mΩ of plasma loading in the (n,m) = (2,1) continuum. An actual minor advantage of the low frequency is that a deposited layer of resistive material, such as is the case with carbonisation, would be relatively transparent at small thicknesses, not leading to an increase in vacuum resistance.

The availability of off-the-shelf technology power sources, relatively inexpensive, is an advantage, as is their reasonable total system efficiency. The tunability of the sources is clearly essential for any active profile control scheme, and within the capabilities of the available technology.

There is no known limit of operation for AWH, in size, field or density. Again the tunability of the power source is essential to cover a wide range of experimental parameters.

The lack of an imposable poloidal purity removes the need for two antennae per toroidal location, since the fully excited m-spectrum will always be dominated by m = -1. This removes the objection that Alfvén Wave Heating antennae must cover the torus wall. The height and number of the antennae can be optimised to match the antenna loading to the maximum permissible feed through current.

The choice of the optimum N-number for a large device has been discussed by many authors, for example Appert and colleagues (1986) and Kirov and colleagues (1985). It appears that going to a higher-N configuration may increase the unit antenna loading in a large machine, thereby increasing the efficiency and decreasing the antenna current compared with the low-N case, which we already consider to be practicable.

It may well be expected that as the size of the machine increases, the problem of impurity release may become negligible, as has already been demonstrated by ICRF experiments.

SUMMARY OF THE CONCLUSIONS

We briefly summarize the conclusions of this review paper as follows:

a) There has been a broad advance in the physics underlying the excitation of Alfvén waves, leading to a better understanding of the importance of the different theoretically predicted effects

b) The observation of the inwardly propagating Kinetic Afvén Waves associated with different resonance layers has filled a gap in the measurements possible in a hot plasma

c) The rf power, up to 570 kW radiated from the antennae, is efficiently absorbed by the plasma, as shown by the enhanced sawtooth activity and also by the peaked radiated power profile at high density ($\bar{n}_e > 6 \times 10^{19} m^{-3}$)

d) Although most power goes to the electrons, a measurable fraction appears to go directly to the ions

e) The large density increase observed during the rf pulse is not composed of impurities by more than 20-30%, the rest being the filling gas

f) Recent results from TCA have shown up changes in the current profile, triggered by particular zones in the excited spectrum. Since the spectrum can be excited at will, by

control of the frequency or the mode, this suggests that an active form of current profile control might be imagined using AWH

g) An increase in particle confinement during the rf pulse has been inferred from the density behaviour

h) No problem has been foreseen in extrapolating AWH to a more powerful tokamak.

ACKNOWLEDGEMENTS

We are grateful for the continued support of the whole TCA team, and well as the stimulation provided by Prof. F. Troyon. The work on TCA was partly funded by the Fonds National Suisse de la Recherche Scientifique.

REFERENCES

Alikaev, V.V., and K.A. Razumova (1985). Course and Workshop on Applications of RF Waves to Tokamak Plasmas, Varenna, Vol. I, 377.

Appert, K., R. Gruber, F. Troyon, and J. Vaclavik (1982). Plasma Phys., 24, 1147.

Appert, K. et al. (1984a). Proc. Invited Papers Int. Conf. on Plasma Physics, Lausanne, Vol. I, 209.

Appert, K. et al. (1984b). Proc. 4th Int. Symp. on Heating in Toroidal Plasmas, Rome, Vol. I, 171.

Appert, K. et al. (1985). Phys. Rev. Lett., 54, 1671.

Appert, K., G.A. Collins, T. Hellsten, J. Vaclavik, and L. Villard (1986). Plasma Phys. Contr. Fusion, 28, 133.

Behn, R. et al. (1984). Plasma Phys. Contr. Fusion, 26, 173.

Behn, R., G.A. Collins, J.B. Lister, and H. Weisen (1986). Proc. 13th European Conf. on Controlled Fusion and Plasma Heating, Schliersee.

Borg, G.G., M.H. Brennan, R.C. Cross, L. Giannone, and I.J. Donnelly (1985). Plasma Phys. Contr. Fusion, 27, 1125.

Bugmann, G. et al. (1981). Proc. 10th European Conf. on Controlled Fusion and Plasma Physics, Moscow.

de Chambrier, A. et al. (1982). Plasma Phys., 24, 893.

de Chambrier, A. et al. (1983). Plasma Phys., 25, 1021.

de Chambrier, A. et al. (1984a). J. Nucl. Mater., 128-129, 310.

de Chambrier, A. et al. (1984b). Helv. Phys. Acta, 57, 110.

de Chambrier, A. et al. (1984c). Proc. 10th Int. Conf. on Plasma Physics and Controlled Nuclear Fusion Research, London, Vol. I, 531.

de Chambrier, A., G.A. Collins, B. Joye, A. Lietti, J.B. Lister, and J.-M. Moret (1985). Proc. 12th European Conf. on Controlled Fusion and Plasma Physics, Budapest, Vol. II, 264.

Collins, G.A., B. Joye, J.B. Lister, and J.-M. Moret (1985). Proc. 12th European Conf. on Controlled Fusion and Plasma Physics, Budapest, Vol. II, 248.

Collins, G.A., F. Hofmann, B. Joye, R. Keller, A. Lietti, J.B. Lister, and A. Pochelon (1986). Phys. Fluids, in press.

Collins, G.A., J.B. Lister, and Ph. Marmillod (1986). Proc. 13th European Conf. on Controlled Fusion and Plasma Heating, Schliersee.

Cramer, N.F., and I.J. Donnelly (1983). Plasma Phys., 25, 703.

Degtyarev, L.M., A.A. Martynov, S.Yu. Medvedev, A.G. Kirov, and M.A. Stotland (1984). Proc. 10th Int. Conf. on Plasma Physics and Controlled Nuclear Fusion Research, London, Vol. II, 156.

Demirkhanov, R.A., A.G. Kirov, L.F. Ruchko, and A.V. Sukachev (1981). JETP Lett., 33, 28.

Demirkhanov, R.A. et al. (1982). Proc. 9th Int. Conf. on Plasma Physics and Controlled Nuclear Fusion Research, London, Vol. II, 91.

Evans, T.E. et al. (1984). Phys. Rev. Lett., 53, 1743.

Hasegawa, A., and L. Chen (1975). Phys. Rev. Lett., 35, 370.

Hofmann, F., K. Appert, and L. Villard (1984). Nucl. Fusion, 24, 1679.

Kirov, A.G., L.F. Ruchko, and A.V. Sukachev (1980). Proc. 2nd Int. Symp. on Heating in Toroidal Plasmas, Como, Vol. II, 689.

Kirov, A.G. et al. (1984). Proc. 10th Int. Conf. on Plasma Physics and Controlled Nuclear Fusion Research, London, Vol. I, 643.

Kirov, A.G. et al. (1985). Proc. 12th European Conf. on Controlled Fusion and Plasma Physics, Budapest, Vol. II, 260.

Lietti, A., and G. Besson (1986). J. Sci. Instrum., in press.

Oakes, M.E., W.D. Booth, P.M. Valanju, and R.D. Bengston (1985). Bull. Am. Phys. Soc., 30, 1593.

Ross, D.W., Y. Li, S.M. Mahajan, and R.B. Michie (1986). Nucl. Fusion, 26, 139.

Shohet, J.L. (1978). Comments Plasma Phys. Contr. Fusion, 4, 37.

Shvets, O.M. et al. (1986). Nucl. Fusion, 26, 23.

Sidorov, V.P. et al. (1983). Proc. 11th European Conf. on Controlled Fusion and Plasma Physics, Aachen, Vol. II, 307.

Taylor, R.J. et al. (1984). Proc. 10th Int. Conf. on Plasma Physics and Controlled Nuclear Fusion Research, London, Vol. I, 581.

Tsushima, A., Y. Amagishi, and M. Inutake (1982). Phys. Lett., 88A, 457.

Villard, L. (1984). private communication.

Weisen, H. (1985). Infrared Phys., 25, 543.

Witherspoon, F.D., S.C. Prager, and J.C. Sprott (1984). Phys. Rev. Lett., 53, 1559.

OBSERVATION OF DENSITY FLUCTUATIONS LOCALIZED AT THE RESONANCE LAYER DURING ALFVEN WAVE HEATING

R. Behn, G.A. Collins, J.B. Lister and H. Weisen

Centre de Recherches en Physique des Plasmas
Association Euratom - Confédération Suisse
Ecole Polytechnique Fédérale de Lausanne
21, Av. des Bains, CH-1007 Lausanne / Switzerland

Abstract

We report on the first observations of density fluctuations at the resonant layer during Alfvén Wave heating in a tokamak. Whereas loading and external magnetic probe measurements[1] show excellent agreement with the cold plasma model of the Shear Alfvén Wave if finite ω/ω_{ci} effects and toroidal coupling are taken into account, these new observations demonstrate the importance of kinetic effects.

Introduction

New insight on the processes underlying Alfvén Wave heating has been gained following the installation on the TCA tokamak of a novel laser diagnostic based on the phase constrast method[2,3,4]. This instrument uses an 8 Watt CO_2 laser beam expanded to fill the 23 x 4 cm wide NaCl windows giving access to the outer two thirds of a poloidal section. The transmitted light is optically processed to produce an image of the plasma, where the small ($\sim 10^{-3}$) phase shifts caused by refractive perturbations are revealed as intensity variations, which are recorded by HgCdTe detectors (Fig. 1). Even though it needs no external reference beam, this method provides an interferometer equivalent response for fluctuations with wavelengths below an adjustable cutoff $\Lambda_c (\Lambda_c < 20\text{cm})$. This is adequate for wavelengths in the centimetric range, as predicted for the kinetic Alfvén Wave in the conditions of TCA. (B_T =1.5 T, Te(0) $\simeq$ 800 eV, $\bar{n}_e$ typically $2\text{-}6.10^{19}\text{m}^{-3}$, R = 0.61m, a = 0.18m, q(a) $\simeq$ 3.2, working gas D_2 or H_2). Each of the eight groups of antennae is fed separately by the 2.5 MHz generator, so that the dominant toroidal (n) and poloidal (m) mode numbers can be determined by their relative phasings. The antennae excite a fast magnetosonic wave, which is heavily damped when the Shear Alfvén Wave resonance condition [1] is met at some radius in the plasma, defining the resonance layer.

At the high temperatures characteristic of the bulk, kinetic theory [5] predicts a strongly damped, radially inwards propagating wave, with a large electrostatic component, that has its wavefield maximum near the resonance layer. Owing to the essentially cylindrical symmetry of the waves, the pattern of line integrated fluctuations is closely related to the original radial wave pattern. The signals from the

detector(s) are mixed with reference signals from the generator to yield the in phase and in quadrature components. From these the relative phase and amplitude of the density fluctuations are calculated.

Results

Figure 2 shows the amplitude and phase in a deuterium plasma obtained with various combinations of antenna phasings refered to by (N,M), when the detector viewed a chord at r/a = 0.33. The spectrum was scanned by increasing the density during the 60 ms RF pulse.

A strong signal is seen shortly after (and sometimes during) the loading peaks of the discrete AW spectrum, signalling the passing of a new resonant layer, sweeping outwards accross the viewing chord as the density rises. The decreasing phase indicates that the interior of the wave is retarded with respect to the outside. Evidence of toroidal coupling from loading measurements [6] is confirmed, eg. (N,M) = (2,1) also excites (n,m) = (2,0) waves. Modes with a poor loading show low level fluctuations. (The same scale was used for the five cases in the figure.) The appearance and disappearance of the resonance surfaces for different excitation structures demonstrates the toroidal mode purity in the continua, as seen in the discrete spectrum by antenna loading measurements [1].

The (n,m) = (4,-1) wave is of particular interest because no (4,-1) discrete Alfvén wave is observed on TCA, showing that these fluctuations appear independently of the discrete spectrum.

Sawteeth activity is often seen to modulate the amplitude and, to a lesser extend, the phase of the signals, indicating the sensitivity of the waves to changes in the plasma profiles. The short scale spikes on Fig. 1 were caused by sawteeth.

The localised radial wave structure and its inward direction of propagation are demonstrated on Fig. 3 obtained from a series of 20 reproducible discharges in hydrogen, where the detector position was scanned from shot to shot (antenna current 630 A peak, 100 kW coupled to the plasma, $n_e = 3.5 \times 10^{19}$). On the contour plot of Fig. 4, we see the detected amplitude as a function of position and density for the same discharges, shown together with the wavefronts (dashed, half-wavelength spacing). The amplitude is seen to be peaked near the estimated (2,0) and (2,-1) resonant layer positions (solid lines). Initial measurements for the (4,-1) continuum show a similar evolution of the profile as a function of density. Unlike the (2,0), the fluctuation level at the threshold is almost zero for the central chord. We attribute this to the difference in poloidal mode number parity.

Conclusions

Using a novel laser diagnostic specifically built for this purpose, we have revealed the existence of driven density fluctuations that have

the features of the Kinetic Alfvén Wave. Further progress is expected from the planned installation of a multi-element detector, which will set us free from the necessity of time consuming repetitive shots to obtain fluctuation profiles.

References

[1] G.A. Collins et al., Phys. Fluids, in press (1986).
[2] H. Weisen, Infrared Phys., 25 (1985) 543.
[3] H. Weisen, Proc. 2nd Int. Symposium on Laser-Aided Plasma Diagnostics, Culham, 10-12 sept. 1985.
[4] H. Weisen, Plasma Phys. Contr. Fusion, in press (1986).
[5] A. Hasegawa, L. Chen, Phys. Rev. Lett., 35 (1975) 370.
[6] K. Appert et al., Phys. Rev. Lett., 54, (1985) 1671.

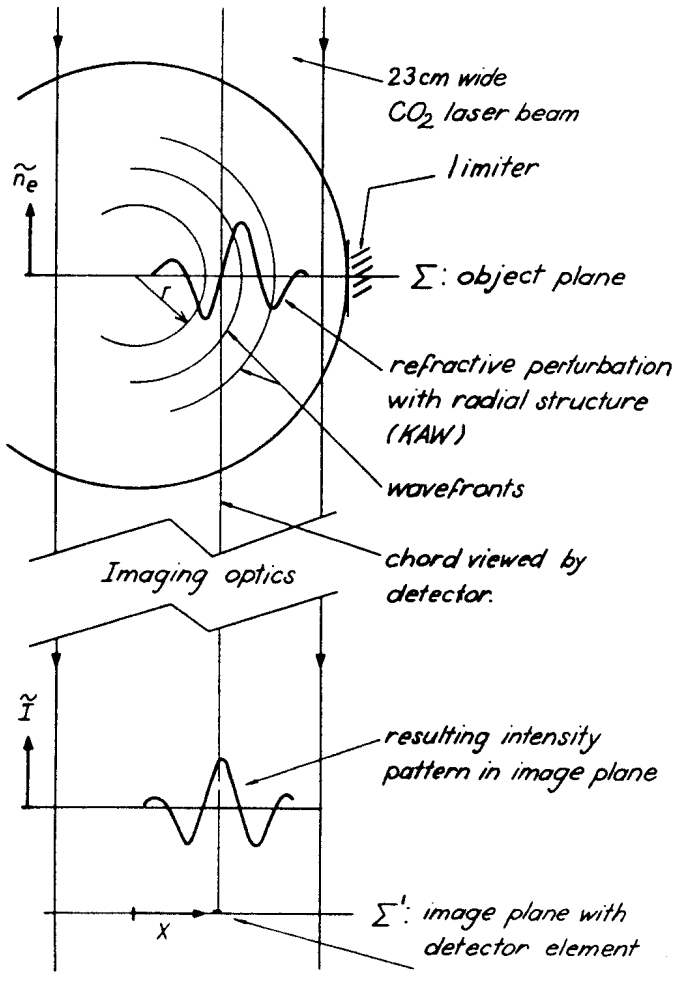

fig.1 Setup

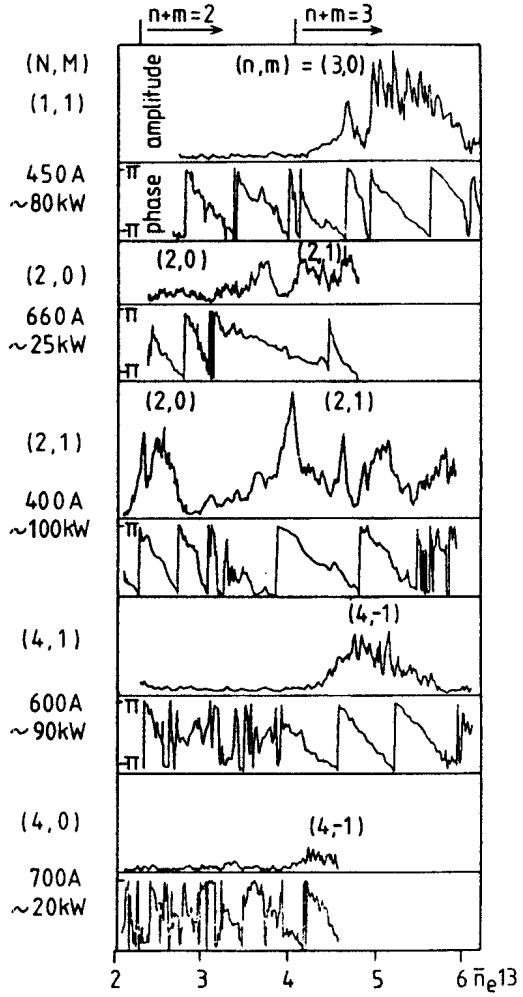

fig.2 (N,M) scan

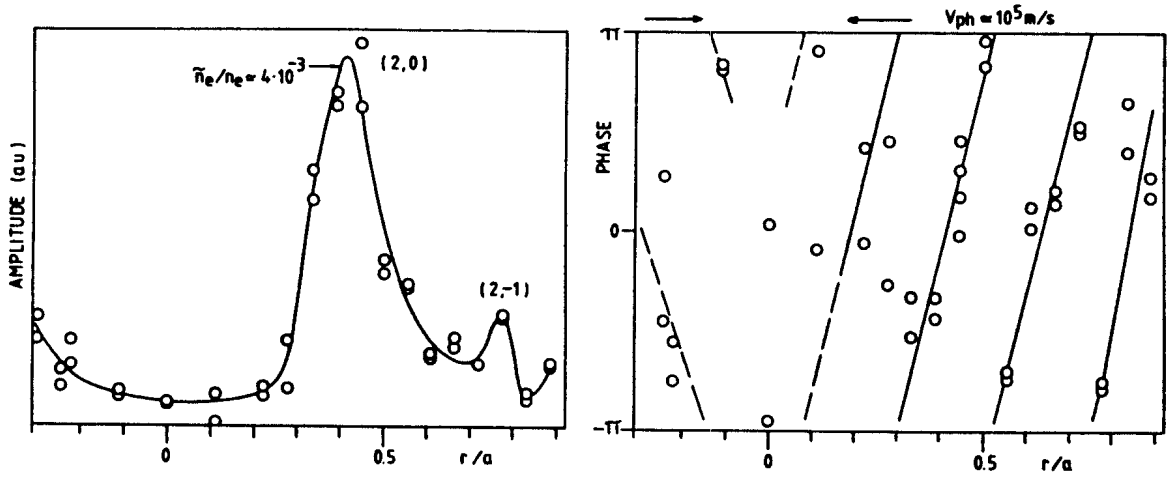

fig. 4 Amplitude and phase profile
(2,0) continuum

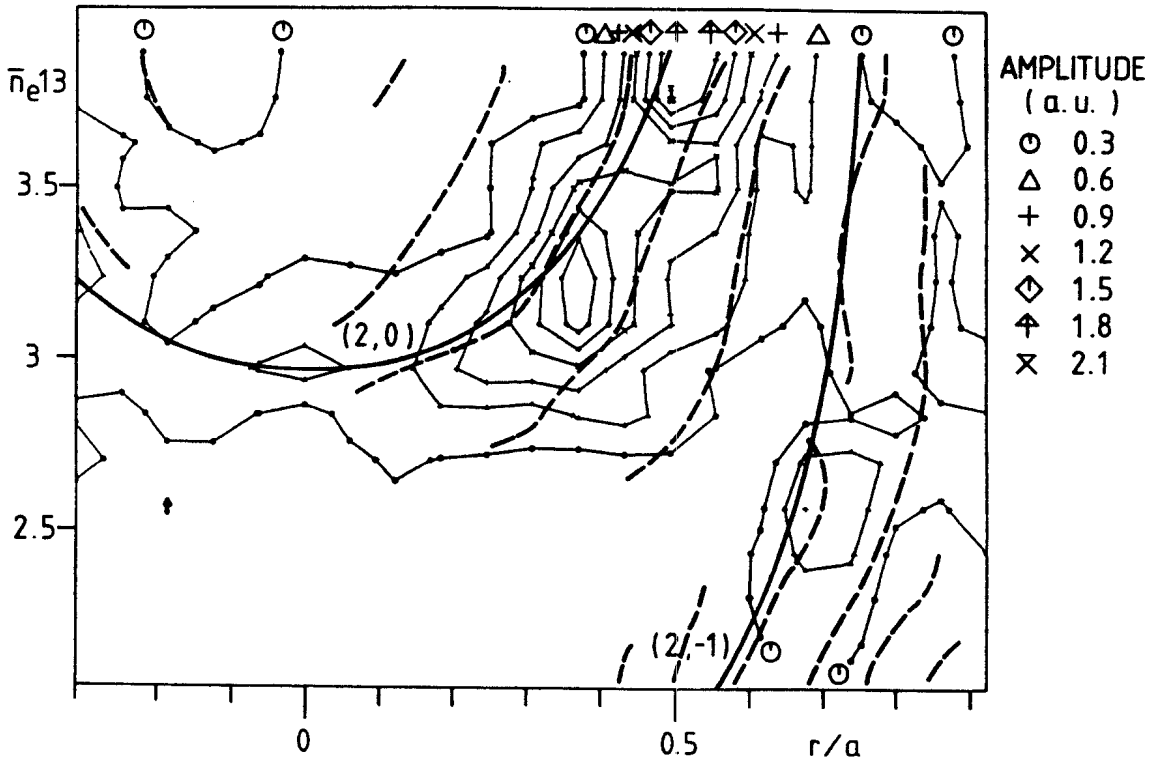

fig. 5 Contour plot

CENTRAL MASS AND CURRENT DENSITY MEASUREMENTS IN TOKOMAKS USING THE DISCRETE ALFVEN WAVE SPECTRUM

G.A. Collins, J.B. Lister and Ph. Marmillod

Centre de Recherches en Physique des Plasmas
Association Euratom - Confédération Suisse
Ecole Polytechnique Fédérale de Lausanne
21, Av. des Bains, CH-1007 Lausanne / Switzerland

We report on the use of global modes of the Alfvén wave to obtain information on the central mass and current density in two tokamaks - TCA and PETULA.

Introduction

For many years the global eigenmodes of both the Alfvén wave and the fast compressional wave have been used as a diagnostic of low temperature plasmas. However their exploitation for the diagnosis of tokamak plasmas has been minimal. Global modes of the fast wave have frequencies that reflect global parameters, such as the average mass density, and, as their popular name "cavity mode" implies, their frequencies are sensitive to the boundary conditions. Even less attention has been given to global modes of the Alfvén wave since it was firmly believed that they only could be excited close to the ion cyclotron frequency ω_{ci}, hence the name Ion Cyclotron Wave. This belief was overturned by the early AWH experiments on TCA which revealed well defined peaks in the antenna loading spectrum at frequencies just below the thresholds of shear Alfvén wave continua, even at values of $\omega/\omega_{ci}<0.1$[1]. A more careful examination of mhd theory indicated that such global modes, labelled as the Discrete Alfvén Wave (DAW), existed at this low frequency due to the presence of the plasma current. This fact and its close association with the continuum threshold, which is usually defined by parameters at the centre of the tokomak discharge, makes the DAW interesting as a tokamak diagnostic [2,3], particularly to have access to information from the core of the discharge, such as the central current density, which is often difficult to obtain. In this paper we give a very brief theoretical background to the information available from the DAW spectrum and describe the experimental installation on two tokamaks - TCA (a=0.18m, R=0.61m, B_ϕ=1.5T) and PETULA (a=0.17m, R=0.71m, B_ϕ=2.8T). We present measurements of the effective mass $A_{eff}(0)$ made during impurity puffing experiments on TCA and estimates of q(0) over a variety of discharges. From PETULA we present preliminary measurements intended to elucidate behaviour of the central current density during LHCD.

Theoretical Background

The shear Alfvén wave continium can be defined for a tokomak plasma in the large aspect ratio approximation as

$$\omega_A(r) = [1/v_A^2(r)\, k_\parallel^2(r) + 1/\omega_{ci}^2]^{-1/2} \qquad (1)$$

where $v_A(r)=B_\phi/[\mu_o\rho(r)]^{1/2}$, $k_\parallel(r)=[n+m/q(r)]/R$ and n, m are the toroidal and poloidal wavenumbers. The continuum threshold ω_{min} is defined by the minimum value of eq.(1) which is usually associated with a radius close to the magnetic axis. We are interested in the first radial eigenmode of the DAW spectrum which occurs at a frequency $\omega_1<\omega_{min}$. Naively we can assume that $\omega_1\sim\omega_{min}\sim\omega_A(0)$ and see from eq.(1) the

dependence of ω_l on both $\rho(0)$ and $q(0)$. In reality the separation $\Delta\omega=\omega_l-\omega_{min}$ also depends on $q(0)$ as well as the ratio ω/ω_{ci} and the actual profiles of $\rho(0)$ and $q(0)$ near the axis. While some analytic approximations exist to predict $\Delta\omega$ for restrictive conditions we prefer to calculate ω_l directly. We remain in cylindrical geometry and restrict ourselves to mhd theory with inclusion of ion cyclotron effects. This theory has proved adequate in predicting DAW frequencies even for those modes that are excited indirectly by toroidal coupling [4].

Experimental Description

Previous studies of the DAW spectrum on TCA have used the AWH antenna structure and the high power generator with its restricted frequency range [5]. For diagnostic purposes we use an antenna consisting of two parallel bars, separated by ~10cm, which encircle a poloidal quadrant either at the bottom of the plasma (TCA) or on the outside (PETULA). A 200 W amplifier provides 1-5A of antenna current via a wideband matching circuit, while detection is made 180° toroidally from the antenna with a magnetic field probe close to the vessel wall and protected by a ceramic tube. A heterodyne detection system allows adequate signal-to-noise with less than 10W coupled to the plasma. A typical scan of 2-10MHz in PETULA is shown in Fig.1. The peaks of the DAW spectrum can be identified by both the amplitude and phase relative to the antenna current. The toroidal field component b_ϕ is used since it is least sensitive to the localised waves that the antenna can excite in the scrape-off. Varying the electron density between discharges and scanning the frequency during 30-70ms allows us to plot the DAW frequencies as a function of line-averaged density, shown in Fig.2 for deuterium discharges in TCA (I_p=125kA) and PETULA (I_p=147kA). Also shown are the theoretical frequencies for constant model density and current profiles. In most cases we have found the dominant peaks to have wavenumbers m=-1 and n<0 since we restrict ourselves to $\omega/\omega_{ci}<0.5$.

Of more interest is the variation in the DAW frequencies. In Fig.3 we illustrate the sensitivity of the technique to variation in central plasma parameters during sawteeth activity in TCA. In this case the frequency was swept slowly over an extremely narrow frequency range to emphasize the change of DAW frequency as revealed by the detected phase. To follow a peak we can either sweep the frequency rapidly (in typically 5ms) over a narrow band around the nominal value, or use the phase information from the detector to track the peak, with a bandwidth up to 10kHz. In Fig.4 we show preliminary results for several peaks measured during LHCD at 3.7GHz in PETULA.

Effective mass during impurity puffing

Injecting a low Z impurity into a hydrogen plasma changes the effective mass $A_{eff}=\sum\eta_i A_i$ from a value close to 1.0 up to a maximum near 2.0 for fully stripped impurities. This lowers the DAW frequency ω_l by decreasing the Alfvén velocity v_A and introducing lower ion cyclotron frequencies ω_{ci}. Calculating the dependence of ω_l on impurity concentration produces the empirical scaling law illustrated in Fig.5. For the magnitude of frequency variations in this case, small variations in the profiles $\rho(r)/\rho(0)$ and $q(r)$ have minimal effect. The use of several peaks increases the accuracy of the measurement. In Fig.6 we show the derived value of $A_{eff}(0)$ for discharges in TCA where the electron density was increased by a factor >3 by the injection of nitrogen. For comparison we also show the value of $A_{eff}(0)$ as a function of density in "pure" hydro-

gen discharges and a predicted curve for $A_{eff}(0)$ if all the increase in electron density is due to nitrogen. Clearly the injection of nitrogen also causes an increase in hydrogen density. Such behaviour is confirmed by measurements of the radiated power profiles. We note for the future that since tritium has an anomalous A/Z=3 this technique offers an accurate way of measuring the D-T mixture as a fusion discharge evolves.

Central current density in Ohmic discharges

We present in Fig.7 the variation in DAW frequency as a function of plasma current in deuterium discharges in TCA (A_{eff}=2.0). As both q(0) and the profile q(r) can be modified by a change in I_p we have calculated the expected dependence for a crude variety of model profiles. FIR interferometer measurements indicate a peaking of $n_e(r)$ as I_p is reduced so this has been included in the calculations. An estimate of q(0) can be made with an uncertainty expressed as being related to q(0.5). Once again the use of several peaks increases the accuracy. In particular low-n DAW's are generally more sensitive to changes in the current profile than those of higher toroidal wavenumber. In Fig.8 we see the variation in DAW frequency at a constant value of I_p but with different values of $\dot{I}_p$. Peaking of the current profile at negative values of $\dot{I}_p$ is reflected in an increase in frequency.

Acknowledgments. We thank the PETULA group for their encouragement to develop this technique and the opportunity to use it on their tokamak. We acknowledge the support of Prof. Troyon and the TCA team, as well as the funding of the Fonds National Suisse.

References

[1] A. de Chambrier et al., Plasma Phys. 24 (1982) 893.
[2] B. Joye et al., "Discrete Alfvén Wave excitation as a tokamak plasma diagnostic", LRP 196/81, Lausanne (1981).
[3] A. de Chambrier et al., Phys. Lett. 92A (1982) 279.
[4] K. Appert et al., Phys. Rev. Lett. 54 (1985) 1671.
[5] G.A. Collins et al., to appear in Phys. Fluids.

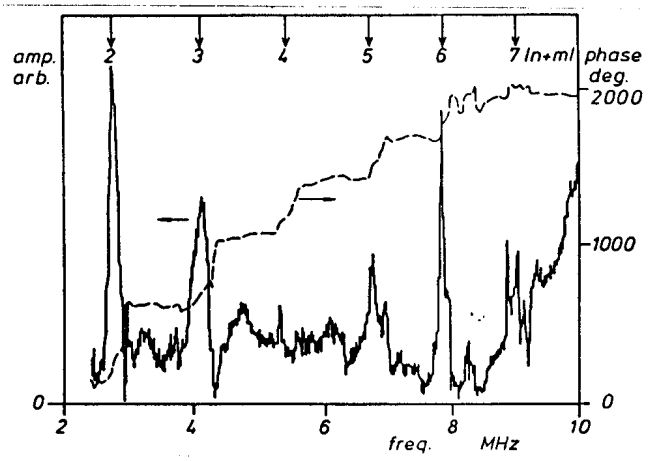

Fig.1 PETULA spectrum(I_p=147kA,$\overline{n}_{e13}$=3)

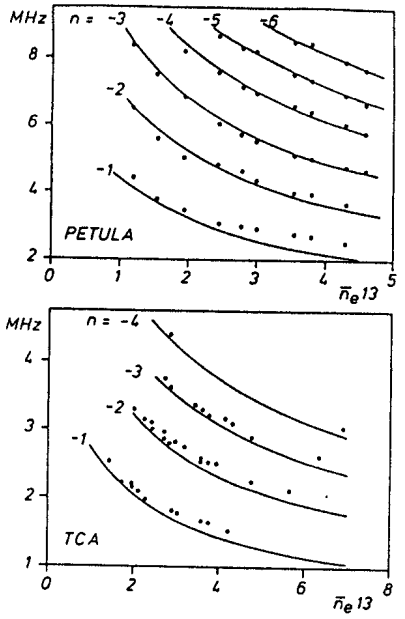

Fig.2 Density scans - measurements and theory(m=-1)

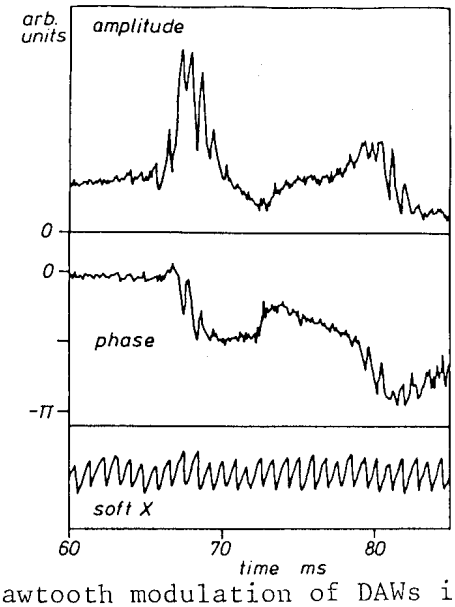

Fig.3 Sawtooth modulation of DAWs in TCA (10kHz/ms, $|n+m|=5$, $I_p=120$kA, $\overline{n}_{e13}=3$)

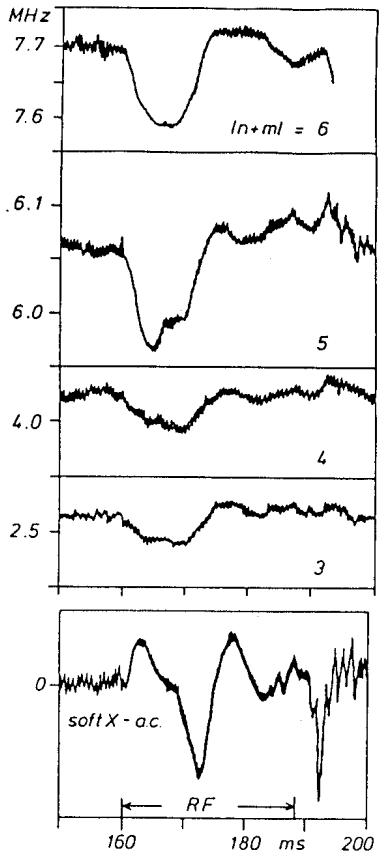

Fig.4 Frequency tracking during LHCD in PETULA

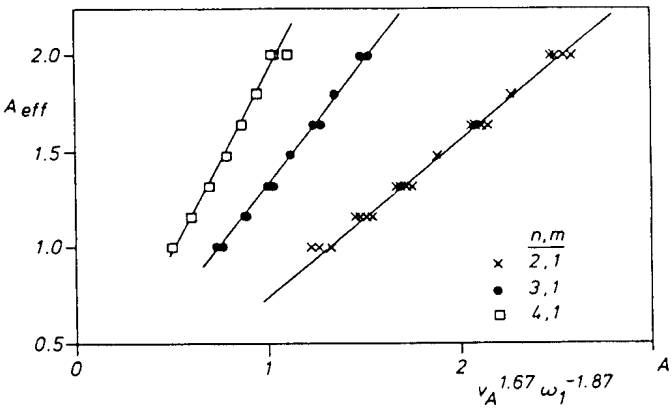

Fig.5 Theoretical scaling law for A_{eff}

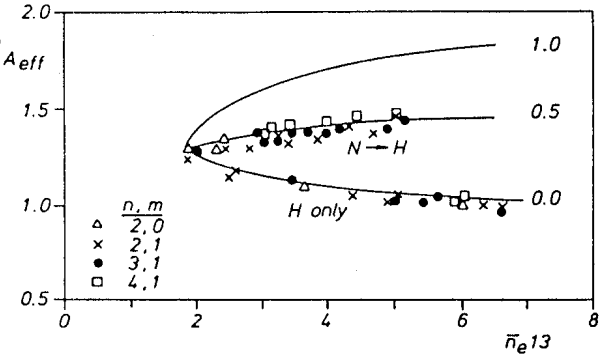

Fig.6 A_{eff} during nitrogen injection Curves calc. for diff. imp. fractions

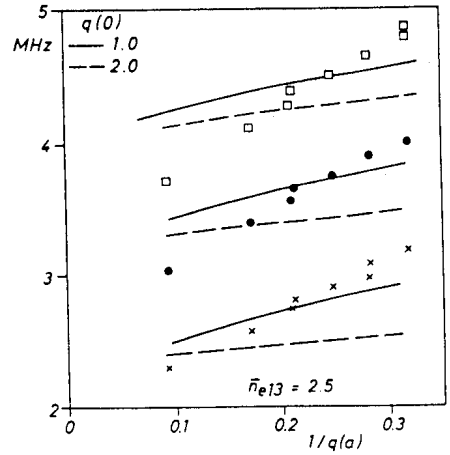

Fig.7 TCA current scan with curves from model profiles

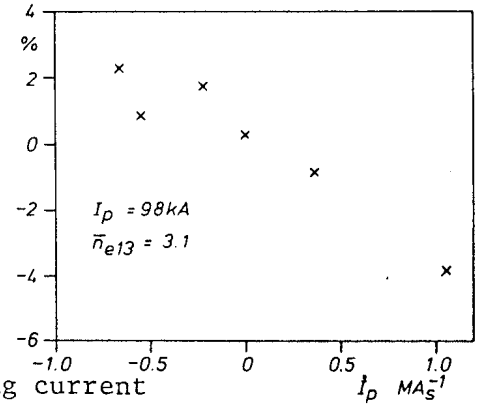

Fig.8 Change in (-2,-1) freq. with ramping current

CHARACTERISTICS OF BROADBAND MAGNETIC AND DENSITY FLUCTUATIONS IN THE TCA TOKAMAK

Ch. Hollenstein, R. Keller, A. Pochelon, M.L. Sawley, W. Simm and H. Weisen

Centre de Recherches en Physique des Plasmas
Association Euratom - Confédération Suisse
Ecole Polytechnique Fédérale de Lausanne
21, Av. des Bains, CH-1007 Lausanne / Switzerland

Abstract

The results of studies of broadband magnetic and density fluctuations during ohmic discharges in the TCA tokamak[1] are described.

Introduction

Three different diagnostics have been employed to investigate the broadband spectrum of fluctuations observed at frequencies greater than the Mirnov frequency (≃ 10kHz in TCA): (i) magnetic probes placed at various poloidal and toroidal locations in the shadow of the limiters, (ii) a triple Langmuir probe for scrape-off plasma measurements, and (iii) a novel CO_2 laser phase contrast diagnostic[2] that yields line-integrated density fluctuations along selected vertical chords of the plasma cross-section.

In Fig. 1 is shown an example of the power spectrum of the magnetic fluctuations. By rotating a probe, ensuring precise measurement of the probe angle with respect to the static field B_ϕ, the fluctuation field has been determined to be polarized in the plane normal to the total magnetic field at the probe position ($\tilde{b}_\parallel/\tilde{b}_\perp \lesssim 10^{-2}$). The level of the magnetic fluctuations, measured 4 cm behind the limiter, is in the range $[\tilde{b}_\theta(f>40kHz)/B_\theta]_{rms} = 10^{-5}$-$10^{-4}$. It is found to scale inversely with energy confinement time, suggesting a possible relation with confinement.[3,4]

The Langmuir probe measurements in the scrape-off layer show a high relative level of fluctuation ($\tilde{n}_e/n_e \simeq 50$-$100\%$). Correlation between the fluctuations in density and potential yields an outward-directed transport, which is dominated by the low frequency contribution (see Fig. 2).[5]

From the phase contrast diagnostic it has been determined that the absolute level of the chord-averaged fluctuations is rather constant for $r/a < 0.5$. This suggests that the fluctuation level is largest in the gradient region ($\tilde{n}_e/n_e \simeq 10\%$ is estimated for $r/a = 0.75$).

Comparison between diagnostics

The results obtained from the three diagnostics can be compared with respect to their spectral and spatial characteristics and also their dependence on the plasma parameters.

All three diagnostics yield power spectra that exhibit an $f^{-\alpha}$ dependence above a roll-off frequency f_c. Spectra determined from the phase contrast diagnostic viewing a central chord are considerably

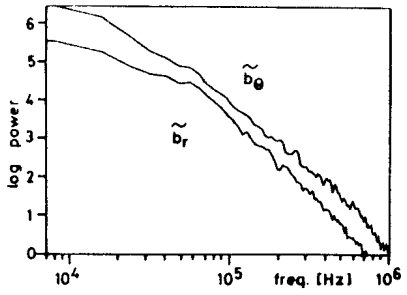

Fig. 1

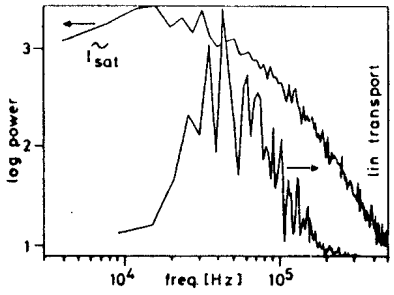

Fig. 2

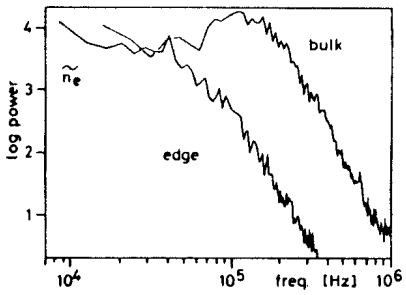

Fig. 3

broader than those obtained from the Langmuir probe, but quite similar for an edge chord that does not probe the bulk plasma (Fig. 3). Figure 4 shows that f_c gradually decreases from ~150kHz for a central chord to the low values (30-80kHz) measured by the Langmuir probe in the scrape-off layer. This figure also shows that the spectral index α for density fluctuations is only weakly dependent on position. The spectral indices for both density and magnetic fluctuations are not strongly dependent on the plasma parameters. (For the parameters of Fig. 4, $\alpha \simeq 3$ for $\tilde{b}_\theta$.)

Correlation measurements using the Langmuir probes yield poloidal phase velocities in the range $1 - 5 \times 10^5$ cm s^{-1} (ion diamagnetic direction), while about 5×10^5 cm s^{-1} is obtained from the phase contrast diagnostic (undetermined direction).

Evidence of significant coherence over long distances has been obtained from both the phase contrast diagnostic and the magnetic probes. Figure 5 shows the spatial autocorrelation function of the density fluctuations obtained from two scannable detectors. For frequencies up to 100 kHz, sizable coherence is observed between chords separated up to 7 cm. In fact, more than half the spectral power of the density fluctuations is associated with long wavelengths; $kr_s = kc_s/\omega_{ci} \lesssim 0.1$ (edge) and $kr_s \lesssim 0.3$ (bulk). These values are comparable to those predicted by strong drift wave models.[6] Although the poloidal coherence length for magnetic fluctuations is only a few centimeters, the examples shown in Fig. 6 demonstrate that significant levels of coherence have been observed from probes in diametrically opposite poloidal ($\Delta\phi=0$, $\Delta\theta=\pi$) and toroidal ($\Delta\phi=\pi$, $\Delta\theta=\pi/2$) planes. This substantial coherence is measured up to ~400 kHz, well above the discernible harmonics of the Mirnov frequency. (A somewhat irreproducible measured phase relation has hampered interpretation in terms of

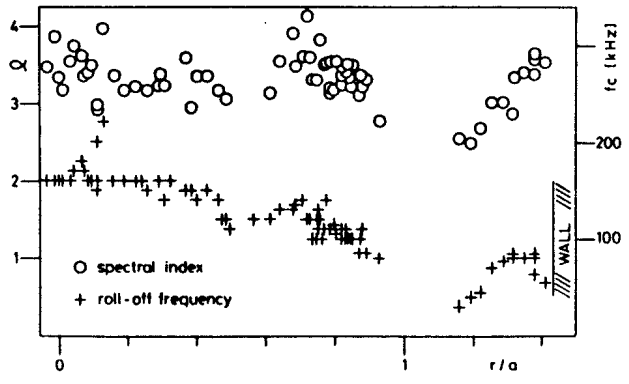

Fig. 4

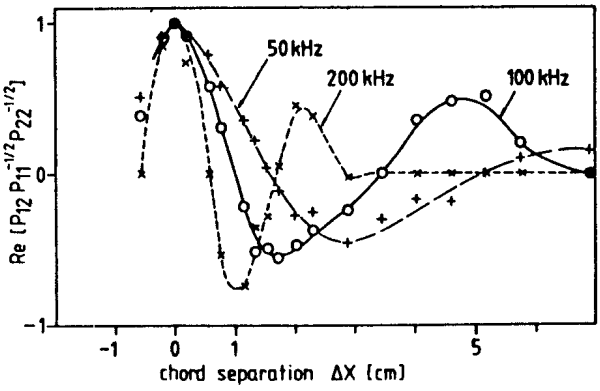

Fig. 5

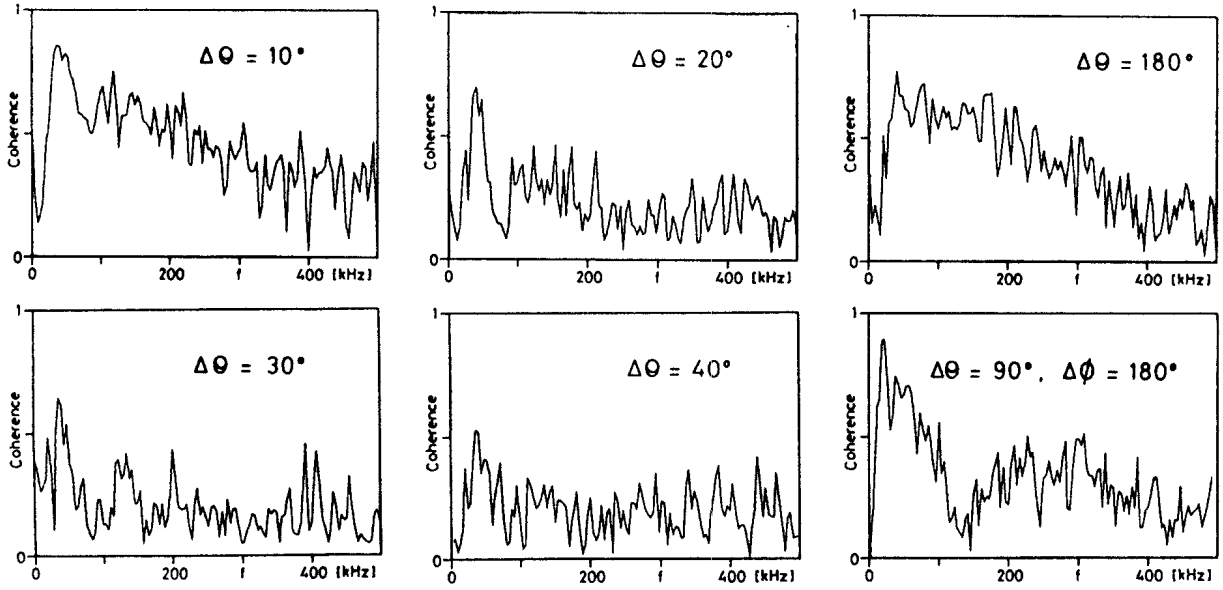

Fig. 6

wave propagation, as for the other two diagnostics.) Despite this observation of long coherence lengths, presumably along the total magnetic field direction, we have found no evidence of significant linear coherence between signals measured by the different diagnostics.[7]

The parametric dependence of the level of density fluctuations measured along a central chord (Fig. 7(a)) constrasts with that measured for $\tilde{b}_\theta$ (Fig. 7(b)). Although $\tilde{n}_e$ increases linearly with n_e, a decrease in $\tilde{b}_\theta$ is measured if n_e is increased. Also, $\tilde{n}_e$ does not exhibit the dependence with plasma current that is observed for $\tilde{b}_\theta$.

Finally, the correlation dimension[8] of the fluctuations has been studied. Signals from each of the three diagnostics, filtered above 40 kHz, yield a high dimension; $\nu > 8$ for the available resolution. For signals containing a large low frequency component, no reliable estimate of the dimension could be obtained.

Conclusions

Long coherence lengths have been measured for both density and magnetic fluctuations. The possible importance of these measurements is stressed by the Langmuir probe results that show that the fluctuation-induced transport is dominated by the long wavelength contribution. Although density and magnetic fluctuations exhibit similar spectral characteristics, no direct connection between them has been observed. The scaling of the density fluctuation level, $\tilde{n}_e/n_e \approx$ constant, does not indicate the same dependence on energy confinement time as measured for $\tilde{b}_\theta/B_\theta$. However, a more definite statement would require detailed measurements of the fluctuation-induced transport in order to determine the role of the observed fluctuations in energy confinement in tokamaks.

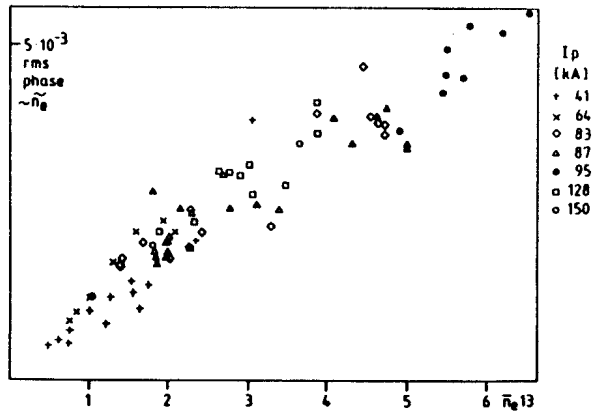

Fig. 7(a)

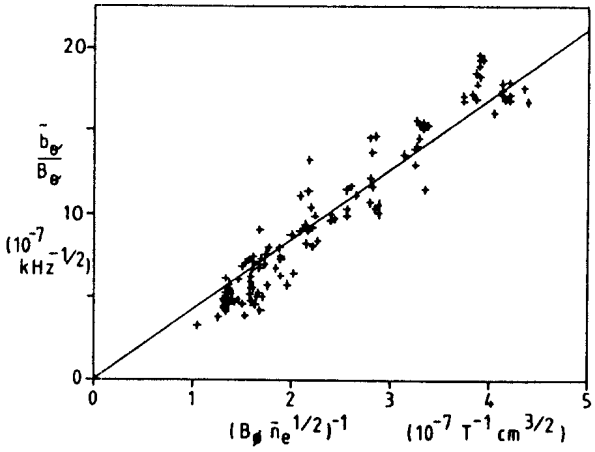

Fig. 7(b)

Acknowledgements

This work was partially supported by the Swiss National Science Foundation.

References

[1] TCA Team, Nucl. Fusion 25, 1041 (1985).
[2] H. Weisen, Infrared Phys. 25, 543 (1985).
[3] P.A. Duperrex et al., Phys. Lett. 106A, 133 (1984).
[4] M.L. Sawley et al., Proc. 12th Europ. Conf. Controll. Fusion and Plasma Phys., Budapest, Vol. I, 291 (1985).
[5] S.J. Zweben et al., J. Nucl. Mat. 111, 39 (1982).
[6] P.C. Liewer, Nucl. Fusion 25, 543 (1985).
[7] S.J. Zweben and R.J. Taylor, Nucl. Fusion 21, 193 (1981).
[8] P. Grassberger and I. Procaccia, Phys. Rev. Lett. 50, 346 (1983).

AXISYMMETRIC, RESISTIVE STABILITY AND CONTROL STUDIES FOR THE PROPOSED TCV TOKAMAK

J. DeLucia,* F. Hofmann, S.C. Jardin,* R. Keller, F.B. Marcus, P. Marmillod and A. Perez
Centre de Recherches en Physique des Plasmas
Association Euratom - Confédération Suisse
Ecole Polytechnique Fédérale de Lausanne
21, Av. des Bains, CH-1007 Lausanne / Switzerland

* Present address: Plasma Physics Laboratory, Princeton University, Princeton, N.J. 08544, U.S.A.

Abstact :

Axisymmetric, resistive plasma stability and control in the proposed TCV tokamak have been studied with the Tokamak Simulation Code, which models the resistive time-scale evolution of a toroidal plasma, including its interaction with the poloidal field coils and the vacuum vessel. Realistic design parameters for the proposed TCV were used to study questions concerning active feedback response times and passive stabilization. It is shown that the plasma can be actively stabilized by power supplies with natural commutation thyristors operating at 100 Hz with 12 pulses.

Introduction :

The Tokamak Simulation Code TSC is described in [1]. With this code, it has been demonstrated [2] that a tokamak plasma can be evolved continuously from a near-circular, cross-section shape to a 4/1 vertically elongated racetrack. All intermediate stages and the final state are stable to axisymmetric MHD modes. The stabilization is provided by the vacuum vessel walls on the ideal time scale and by an orthogonal active feedback system on the resistive time scale.

In subsequent studies with this code, it was found that the use of either a continuous vacuum vessel or a vessel with a toroidal gap resulted in very similar plasma evolutions. Also, the effects of diagnostics ports were studied by removing short poloidal sections from the toroidal symmetric vessel at port locations. Ideal stability was preserved, and the resistive growth rates did not significantly change. Based on these results, the vessel model used in the studies reported here is continuous poloidally and toroidally, with a resistivity equivalent to 1.0 cm thick INCONEL vessel walls plus strengthening ribs. In previous studies, the shaping coil supplies were ideal current sources. In what follows, the power supplies are natural commutation thyristor rectifiers, and the shaping coils are given the design values of resistance.

Feedback model for voltage source power supplies

For each shaping coil i at any instant of time t, the desired current I (i, t) is given by I (i, t) = $\sum$F(i, t, L) + C (i, t), where C (i, t) is the preprogrammed current to give the desired equilibrium and F (i, t, L) = G (i, L) E (t, L). For values of L=1-4, the coils produce radial, quadrupole, octupole, and vertical fields due to the current distribution G(i,L), which includes a gain factor. The error measurement E(t,L) is obtained by multiplying a state vectror for each of the four control systems by the flux loop measurements. The state vectors for the error measurements and resultant fields are othogonal, so that each feedback system is relatively independent of the others.

At any given instant of time, the difference D(i,t) between the desired current I(i,t) and the actual coil current I*(i,t) is D(i,t)≡I(i,t)-I*(i,t). The plasma and coil current solver in TSC advances the currents during a small time interval dt. We need to specify the coil voltage during this interval, V(i,t+dt) = V(i,t) + dV(i) where V(i,t) is the applied voltage during the previous interval and the change in voltage dV(i) us given by the feedback equation :

$$\frac{dV(i)}{dt} = A_I(i)\,\frac{V^{MX}(i)}{T(i)}\left[D(i,t)+A_P(i)\frac{dD(i,t)}{dt}+A_D\frac{d^2D(i,t)}{dt^2}\right]$$

where A_I, A_P, A_D are the integral, position, and differential gains for each coil, and $V^{MX}(i)$ and T(i) characterize the voltage source power supplies. $V^{MX}(i)$ is the maximum positive or negative voltage, and T(i) is the half-period, corresponding to the time to swing from maximum positive to maximum negative voltage. The command voltage from the feedback equation is therefore limited by

$$|V(i,t)| < V^{MX}(i) \quad \text{and} \quad \left|\frac{dV(i)}{dt}\right| < \frac{2V^{MX}(i)}{T(i)}$$

The resulting command voltage is applied to a model describing an ideal natural-commutation thyristor rectifier power supply for each coil. The thyristor supplies are taken to be 12 pulse and 100 Hz, which allows a commutation every 0.83 msec on average.

Results

The resistivity of each vacuum vessel element is 0.02*R ohms and the global value is 10^{-4} ohms, corresponding to 1.0 cm thick INCONEL plus strengthening ribs. The maximum supply voltages $V^{MX}(i)$ are 25 V/turn for outside coils, and 12.5 V/turn for the inner coils, correponding to the difference in self-inductances. (We note that because the coil grid size is 2.5 cm × 2.5 cm, the coils' self-inductances are larger than in the actual experiment.) For the inner coils (small major radius), the feedback coefficients are A_I = .00064/Amp, A_P = .004 sec, A_D = 0; for the outer coils A_I = .00024/Amp, A_P = .008 sec, A_D = 0. The plasma parameters for the simulation are central density and temperature $3 \times 10^{20} m^{-3}$ and 900 eV, safety factor ratio q_{edge}/q_0 = 2, and toroidal

field 1.5 Tesla. The Alfvén time is artificially enhanced by a factor of 600, so that the Alfvén time is still much less than the vessel time constant.

Examples of the results of a simulation with the above parameters are shown in Fig. 1. The plasma evolves from an elongation of 1.6 up to nearly 2.0 during 60 msec. A sample equilibrium is shown, with the positions of coils #7 and #8 indicated. The applied voltages and resulting coil currents are shown in Fig. 1 as a function of time. The initial conditions have the correct currents for the initial equilibrium, but the voltages are the resitive voltages only, and the plasma current density is not in resistive equilibrium. Thus the feedback model causes a large overshoot in the applied voltages as the plasma begins to evolve, but these are damped out later in time. An oscillation remains, superposed on the thyristor waveforms, because optimal feedback coefficients have not yet been determined.

Conclusions

The plasma is maintained in equilibrium for many 10's of milliseconds, whereas without feedback, it goes unstable on the millisecond time scale, indicating that the system response time is sufficient for the conditions considered.

Acknowledgements : We wish to thank Professor F. Troyon, Dr. R. Gruber and Dr. N. Pomphrey for useful discussions and comments. This work was partly supported by the Swiss National Science Fondation and by the U.S. Department of Energy through contract No. DE-AC02-76-CHO-3073.

References

[1] S.C. Jardin, Computational Techniques, ed. by B. Cohen and J. Brackbill (Academic, New York, 1985).

[2] F.B. Marcus, S.C. Jardin and F. Hofmann, Phys. Rev. Lett. 55, 2289 (1985).

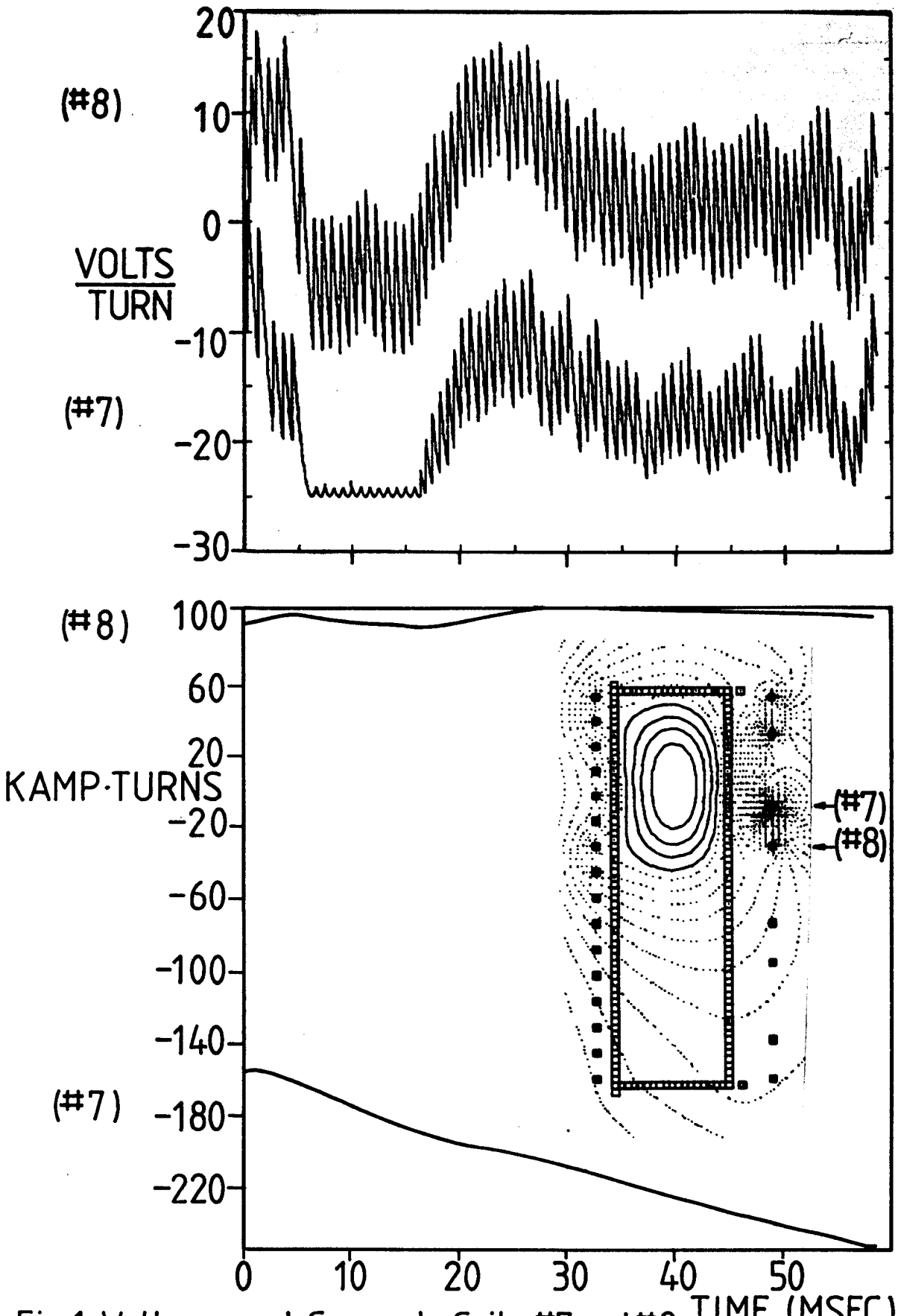

Fig.1 Voltage and Current, Coils #7and #8